JOURNAL OF MATERIALS SCIENCE 8 (1973) 980–992

Extensional and shear compliances of polyethylene terephthalate sheets with orthorhombic symmetry

N. H. LADIZESKY*, I. M. WARD
Department of Physics, Leeds University, UK

The St Venant relations are applied to obtain the three shear compliances of a polymer sheet with orthorhombic symmetry. The results for one way drawn polyethylene terephthalate sheet taken in conjunction with data for two extensional compliances, suggest that in this material, planar orientation is an important factor in determining the mechanical properties.

1. Introduction

In this paper we describe the determination of the three shear compliances of one way drawn polyethylene terephthalate sheets, together with the measurement of the two extensional compliances in the plane of the sheet. The determination of the shear compliances involves the application of the St Venant theory for the torsion of rectangular prisms. Because sheet of one thickness only was available, special procedures had to be devised and these will be described in detail. To our knowledge this is the first time that all three shear compliances of an orthorhombic sheet have been directly determined.

Polyethylene terephthalate sheets, stretched at constant width, possess orthorhombic symmetry, as revealed by optical birefringence and wide-angle X-ray diffraction measurements. The precise structure of these sheets is complicated for two principal reasons. Firstly, there is a considerable distribution of molecular orientation even in the 5:1 draw ratio sheet used in these experiments, and only about 35% of the material shows three-dimensional crystalline order. Secondly, polyethylene terephthalate has a triclinic unit cell [1], which makes for considerable complications in the description of the orientation of the structure. It can be said, however, that these 5:1 sheets have high chain axis orientation in the draw direction, which is shown by the preferred orientation of the crystallographic c-axes and the high refractive index in this direction; and, moreover, that there is preferred orientation of the (100) planes in the crystalline regions such that these lie in the plane of the sheet. The (100) plane is nearly, but not quite, the plane containing the benzene ring of the terephthalate structure.

2. Theory

2.1. Elastic constants

The mechanical properties of an anisotropic elastic solid can be described by a generalized Hooke's law relating strains ϵ_p with stresses σ_q by the following relations:

$$\epsilon_p = S_{pq}\,\sigma_q \qquad \sigma_q = C_{qp}\,\epsilon_p$$

where S_{pq} and C_{qp} are the compliance and stiffness constants respectively and p, q take values 1, 2, . . . 6. These representations are equivalent, but, for convenience, we will work in terms of the compliance constants.

A solid with orthorhombic symmetry has nine independent elastic constants. If we choose the 1, 2, 3 axes as the principal axes of symmetry (Fig. 1), we write the compliance matrix as

$$S_{pq} = \begin{pmatrix} S_{11} & S_{12} & S_{13} & 0 & 0 & 0 \\ S_{12} & S_{22} & S_{23} & 0 & 0 & 0 \\ S_{13} & S_{23} & S_{33} & 0 & 0 & 0 \\ 0 & 0 & 0 & S_{44} & 0 & 0 \\ 0 & 0 & 0 & 0 & S_{55} & 0 \\ 0 & 0 & 0 & 0 & 0 & S_{66} \end{pmatrix}$$

It is to be noted that S_{12}, S_{44}, etc. are terms of the compliance matrix, but they are not the fourth rank tensor compliances.

*Now at School of Applied Sciences, Universiti Sains Malaysia, Minden, Penang, Malaysia.

S_{11}, S_{22} and S_{33} are extensional compliances.
S_{44}, S_{55} and S_{66} are shear compliances.
S_{12}, S_{13} and S_{23} are compliances which involve Poisson's ratios.

2.2. Determination of shear compliances

The shear compliances are determined in torsion experiments by relating a known torque and twist with the shear compliances of the material. The relations are given by the St Venant theory, which is discussed in detail elsewhere [2, 3]. Here it will be sufficient to say that, for a prism with rectangular cross-section possessing orthorhombic symmetry, the six relationships are (referred to a co-ordinate system as shown in Fig. 1)

$$M_z = \frac{ab^3}{S_{55}}\beta(u_z) = \frac{ba^3}{S_{44}}\beta(u_z') \qquad u_z = (u_z')^{-1} = \frac{a}{b}\sqrt{\left(\frac{S_{55}}{S_{44}}\right)}$$

$$M_y = \frac{ac^3}{S_{66}}\beta(u_y) = \frac{ca^3}{S_{44}}\beta(u_y') \qquad u_y = (u_y')^{-1} = \frac{a}{c}\sqrt{\left(\frac{S_{66}}{S_{44}}\right)}$$

$$M_x = \frac{bc^3}{S_{66}}\beta(u_x) = \frac{cb^3}{S_{55}}\beta(u_x') \qquad u_x = (u_x')^{-1} = \frac{b}{c}\sqrt{\left(\frac{S_{66}}{S_{55}}\right)}$$

where M_z, M_y and M_x are the torques applied to a sample of unit length to produce a unit twist around the z, y or x directions respectively, and a, b and c are the sides of the sample parallel to x, y and z respectively.

For the St Venant theory to be applicable, x, y and z must be the principal axes of the orthorhombic sheet. $\beta(u)$, the St Venant function, is

$$\beta(u) = \frac{32}{\pi^4}u^2 \sum_{k=1,3,5,\ldots}^{\infty} \frac{1}{k^4}\left(1 - \frac{2u}{k\pi}\tanh\frac{k\pi}{2u}\right)$$

and is shown in Fig. 2 for $u \geqslant 1$. Only the form of the St Venant relationships giving u (or u') $\geqslant 1$ is used.

Each of the above relations include two shear compliances. Since we do not know any of them, we must use the "pseudo-isotropic" method described in our previous paper [3]. Briefly, this consists in assuming the sample to be transversely isotropic in, say, the xy plane. In this case, $S_{55} = S_{44}$ and if $a/b \gg 1$ we have

$$M_z = \frac{ab^3}{S_{55}}\beta(u_z) \qquad u_z = \frac{a}{b}\sqrt{\left(\frac{S_{55}}{S_{44}}\right)} \simeq \frac{a}{b}.$$

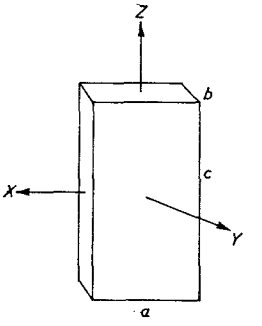

Figure 1 Diagram showing the set of Cartesian axes with respect to sample (c is parallel to initial draw direction, a is perpendicular to the plane of the sheet and normal to c).

The error in u_z produced by this assumption will reflect in S_{55} through $\beta(u_z)$, but Fig. 2 shows that if the true $u_z > 10$, then the error in $\beta(u_z)$ is small. Thus, if a/b is sufficiently large, $\beta(u_z)$ is not sensitive to the value of S_{55}/S_{44} and we may put $\beta(u_z) = 0.32$. A plot of S_{55} versus a/b (S_{55} calculated with the pseudo-isotropic method) can then be extrapolated to $a/b \gg 1$ to find the true value of S_{55}.

In this paper, $S_{55}{}^z$ and $S_{55}{}^x$ will denote particular values of S_{55} calculated from a torsion experiment at a single aspect ratio, for torsion around z and x respectively. $\overline{S_{55}{}^z}$ and $\overline{S_{55}{}^x}$ are the values of $S_{55}{}^z$ and $S_{55}{}^x$ obtained with any method of handling the St Venant theory using the extrapolation techniques. The final value of S_{55} is obtained by combining results from the different methods.

2.3. Calculation of S_{55}

Because the commercially available sheets have a thickness (b dimension) of 0.025 cm, only twists

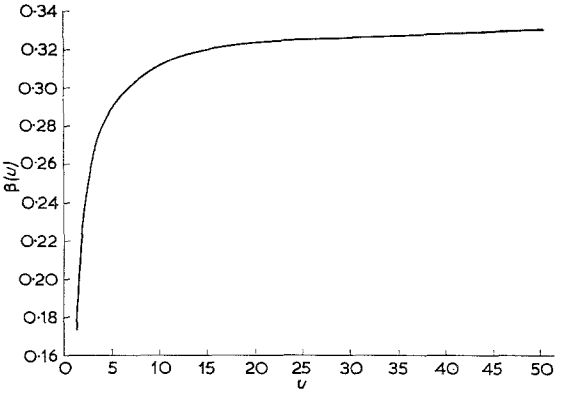

Figure 2 Plot of St Venant's function $\beta(u)$ versus u.

in the z and x directions are possible. The samples will all be such that:

$$\frac{c}{b} > 1 \text{ and } \frac{a}{b} > 1$$

and the two relations to be used experimentally are:

$$M_x = \frac{cb^3}{S_{55}}\beta(u_x) \qquad u_x = \frac{c}{b}\sqrt{\left(\frac{S_{55}}{S_{66}}\right)} \quad (1)$$

$$M_z = \frac{ab^3}{S_{55}}\beta(u_z) \qquad u_z = \frac{a}{b}\sqrt{\left(\frac{S_{55}}{S_{44}}\right)}. \quad (2)$$

It follows that the "pseudo-isotropic" method can only determine S_{55}. We will now consider the relationships between $S_{55}{}^z$, $S_{55}{}^x$ and the aspect ratios, according to the relative values of S_{44}, S_{55} and S_{66}. Four cases can be distinguished:

(a) S_{66} and $S_{44} > S_{55}$
(b) S_{66} and $S_{44} < S_{55}$
(c) $S_{66} > S_{55}$; $S_{44} < S_{55}$
(d) $S_{66} < S_{55}$; $S_{44} > S_{55}$.

Cases (a) and (b) have two possibilities each, namely

$$S_{66} > S_{44} \text{ or } S_{66} < S_{44}.$$

(a) S_{66} and $S_{44} > S_{55}$
In this case:

$$\frac{S_{55}}{S_{66}} < 1 \qquad \frac{S_{55}}{S_{44}} < 1$$

i.e.

$$\frac{c}{b} > u_x \qquad \frac{a}{b} > u_z$$

which means:

$$S_{55}{}^x > S_{55} \qquad S_{55}{}^z > S_{55}.$$

Because of the shape of $\beta(u)$ versus u, the difference between either $S_{55}{}^x$ or $S_{55}{}^z$ and S_{55} is smaller the higher the aspect ratio, that is, $S_{55}{}^x$ and $S_{55}{}^z$ decrease towards S_{55} for increasing aspect ratios.
(a_1) $S_{66} > S_{44}$
In this case:

$$\frac{S_{55}}{S_{66}} < \frac{S_{55}}{S_{44}} < 1.$$

Therefore, the errors produced by taking the aspect ratio instead of the corresponding u are smaller for u_z than for u_x.
i.e. $S_{55}{}^x > S_{55}{}^z > S_{55}$.
(a_2) $S_{66} < S_{44}$
In this case:

$$\frac{S_{55}}{S_{44}} < \frac{S_{55}}{S_{66}} < 1$$

giving $S_{55}{}^z > S_{55}{}^x > S_{55}$.
Similar arguments apply to cases (b), (c) and (d). Summarizing

(a) $S_{66} > S_{55} < S_{44}$
$S_{55}{}^z$ and $S_{55}{}^x$ decrease with increasing aspect ratio, the limit being S_{55}.
If $S_{66} > S_{44}$, then $S_{55}{}^x > S_{55}{}^z > S_{55}$.
If $S_{66} < S_{44}$, then $S_{55}{}^z > S_{55}{}^x > S_{55}$.

(b) $S_{66} < S_{55} > S_{44}$
$S_{55}{}^z$ and $S_{55}{}^x$ increase with increasing aspect ratio, the limit being S_{55}.
If $S_{66} > S_{44}$, then $S_{55}{}^z < S_{55}{}^x < S_{55}$.
If $S_{66} < S_{44}$, then $S_{55}{}^x < S_{55}{}^z < S_{55}$.

(c) $S_{66} > S_{55} > S_{44}$
$S_{55}{}^x$ decreases and $S_{55}{}^z$ increases with increasing aspect ratio, the limit being S_{55}.
In this case:
$S_{55}{}^z > S_{55} > S_{55}{}^x$.

(d) $S_{66} < S_{55} < S_{44}$
$S_{55}{}^x$ increases and $S_{55}{}^z$ decreases with increasing aspect ratio, the limit being S_{55}.
In this case:
$S_{55}{}^z < S_{55} < S_{55}{}^x$.

2.4. Calculation of S_{66} and S_{44}

Once S_{55} is known, we can use relations 1 and 2 (the only ones available to us) to calculate the remaining shear compliances S_{66} and S_{44}. This has been called the "exact" method in reference 3 and it consists in calculating $\beta(u)$ with the known value of S_{55}.

$$\beta(u_x) = \frac{M_x S_{55}}{cb^3} \qquad \beta(u_z) = \frac{M_z S_{55}}{ab^3}.$$

Fig. 2 then provides u_z and u_x, whence

$$S_{66} = \left(\frac{c}{b}\right)^2 \frac{S_{55}}{u_x{}^2}, \qquad S_{44} = \left(\frac{a}{b}\right)^2 \frac{S_{55}}{u_z{}^2}.$$

As discussed previously [3], it was found necessary to extrapolate to $c/b \to 0$ and $a/b \to 0$ to obtain the true values of the shear compliances. In fact, these extrapolations are equivalent to:

$$\frac{b}{c} \to \infty \text{ and } \frac{b}{a} \to \infty$$

which are the conditions for calculating S_{66} and S_{44} as if the sample were transversely isotropic. More details of this will be given later in the paper.

2.5. Correction for axial tensile stress

The St Venant theory assumes that the sample is subjected to a twisting moment only, whereas there is usually also a small tensile stress. The effect of axial tensile stress is to produce an apparent increase in the torsional rigidity. This was first observed in thin metallic strips used as galvanometer suspensions [4, 5]. For a very thin strip, the additional couple can be calculated on the basis that it is similar to a bifilar suspension [6]. A more general treatment later given by Biot [7] showed that the torsional rigidity is increased by a term which is proportional to the polar moment of inertia of the cross-section, with respect to its centre of gravity. Biot's treatment is valid for the case where the plane perpendicular to the twist axis is isotropic. It has been shown in our previous publication [3] that the Biot correction cannot be used in orthorhombic sheets and the St Venant torque must be obtained by an empirical extrapolation to zero axial stress.

3. Experimental

3.1. Preparation of specimens

The samples used were taken from a roll of polyethylene terephthalate sheet, drawn to draw ratio 5:1 at constant width and manufactured by Imperial Chemical Industries Ltd, Plastics Division, Welwyn Garden City. The sheet was several yards long, 50 cm wide and had a thickness varying between 0.023 and 0.045 cm from one edge to the other. All the experiments were confined to samples taken from a 7 cm wide strip, cut 3 cm off the thinner edge.

Samples were always prisms of rectangular cross-section. The dimensions of those used for extensional measurements were $3.5 \times 0.2 \times 0.025$ cm, while those used for torsion measurements were 3.5 cm long, 0.025 cm thick with widths varying between 0.1 and 0.6 cm.

Some difficulties were experienced when cutting the samples. The standard technique was by means of a surgical blade running along a metal ruler. The plastic deformation produced by the cutting seemed to relax the edge of the sample outside the ruler and produce a protuberance along its length with a height of 30% the thickness of the sample. In a 0.1 cm width sample this protuberance can have a cross-sectional area of about 8% the cross-section of the sample, and, although this extra area can be accurately measured, its mechanical properties are unknown. Furthermore, since the applicability of the St Venant theory depends on each side of the prism being parallel to a plane of structural symmetry, the edge protuberance adds non-measurable error to the calculation of the shear compliances.

It was found that the best way to avoid the formation of the protuberance was to cut the samples in such a way that each edge was under the metal ruler, that is, under a high hand pressure. Briefly, this was done by cutting one edge in the standard way, drawing a line parallel to it and then, with the sample under the ruler, cutting the other edge parallel to the line. With practice, an accuracy of 2 to 3% can be achieved in the parallelism of a sample 3.5 cm long and 0.1 cm wide.

Another standard method for obtaining samples was by using a dumbell cutter between the plates of a press. This method gave good samples in the draw direction, but for samples perpendicular to it, the protuberance was significant.

3.2. Torsion measurements

The torsion apparatus was described in detail in reference 2 and only a summary of the method will be given here.

A torque is applied to the sample by means of a 6% phosphor bronze long ($\simeq$ 100 cm) ribbon of known torsional rigidity. If c' is the torque for unit twist per unit length of the suspension, ϕ_{susp} and l_{susp} the twist and length of the suspension, respectively, M_x' the experimental torque for unit twist per unit length of the sample (with an axial stress different from zero) and ϕ_{samp} and l_{samp} the twist and length of the sample, respectively, then

$$\frac{c'\,\phi_{\text{susp}}}{l_{\text{susp}}} = \frac{M_x'\,\phi_{\text{samp}}}{l_{\text{samp}}}.$$

Thus, a graph of M_x' versus axial stress can be made and M_x found by extrapolation. M_z is found in a similar manner.

c' is obtained by attaching inertia bars to the end of the suspension and timing the period, T, of free oscillations. Under these conditions,

$$c' = \frac{4\pi^2 I}{T^2}\, l_{\text{susp}}$$

where I is the moment of inertia of the bar relative to the axis of oscillation.

The remarks concerning the effects of axial stress on the sample (Section 2.5) also apply to the phosphor bronze ribbon. Here the situation

is complicated by the very large strains involved so that the torsional rigidity is a function of both the amount of twist and the axial stress. A graph of c' versus axial load was, therefore, constructed for different twist amplitudes, and the correct value of c' for a given M_x' (or M_z') measurement obtained by interpolation. In practice, the effect of axial load was found to be larger than the effect of twist.

3.3. Extensional compliance apparatus

Extensional compliances were determined using the dead-loading creep apparatus described by Gupta and Ward [8]. The only modification was the fitting of a larger micrometer head, increasing the accuracy of the reading to 5×10^{-5} cm.

3.4. Experimental conditions

The experiments were undertaken in a thermostatically-controlled room at a temperature of $20 \pm 1°C$.

To ensure reproducibility in the torsion experiments, the specimens were conditioned under the maximum axial stress and torque to be used, with two twisting cycles at each side of the equilibrium position. Each cycle consisted of 10 sec maximum torque, followed by 100 sec under approximately zero torque.

Conditioning of the specimens for the extensional compliance experiments consisted of two cycles of 10 sec loading at the maximum load to be used, followed by 100 sec recovery under zero load.

The time-dependence of the extensional and shear compliances was determined up to 1000 sec. As the time-dependences were small and are not of particular interest in the present work, the results will, in general, be given in terms of 10 sec compliances. In the torsion experiments, results were obtained for twists of 0.18 and 0.33 radians.

For a cylinder of diameter 5 mm and length 3.5 cm, a twist of 0.3 radians corresponds to a maximum shear strain of 2.5%. This would be similar to the largest aspect ratio specimens, but the final values of the shear compliances were always obtained, as explained above, by extrapolation to zero aspect ratio from data for a range of aspect ratios. The most important results from the viewpoint of the final extrapolated values are therefore those at lower aspect ratios where the maximum shear strains are lower by almost an order of magnitude. In fact, results for twists of 0.18 and 0.33 radians were within experimental error, and the extensive data reported in this paper are for the higher level of twist because they are considered to be more accurate.

3.5. Experimental errors

In a previous publication [9] it was shown that the extensional compliances can be measured to within $\pm 1.5\%$ but the variability among the present samples was about $\pm 4\%$. It has been said that the thickness of the sheet varies between 0.023 and 0.045 cm from one edge to the other. This was accompanied by 20% variability in S_{33}, but much smaller for S_{11}. The $\pm 4\%$ variability of the extensional compliances as mentioned above refer to samples taken from the 7 cm wide strip referred to in the experimental section.

In the previous work [3] it was found that the experimental spread in the determination of the shear compliances was 10 to 15%. In the present experiments, variability between samples and the use of the extrapolation procedures, as well as some possible departure of our sheets from orthorhombic symmetry, gave a somewhat large range, about 25%.

4. Results

4.1. Calibration of the suspension

Fig. 3a shows c' versus axial load for one of the suspensions used. (0.2×0.005 cm cross-section, 100 cm long). Curves are given for different amplitudes and it can be seen that a linear relationship is a good approximation for all the results

$$c' = A + BW$$

where W is the axial stress and A and B, shown in Fig. 3b, are functions of the amplitude. Thus, c' can be calculated for any axial stress and any twist within the range of the calibration.

4.2. Calculation of the St Venant Torque

Fig. 4 shows M_z' versus axial stress for a 0.5 cm wide sample and a twist of 0.33 radians. It also shows the corresponding torques at zero axial load calculated with the Biot correction (M_z^B). As expected, it is seen that the Biot correction does not produce correct values of M_z.

Fig. 5 shows similar results for M_x' versus axial stress for a 0.4 cm wide sample.

4.3. Calculation of S_{55}

Fig. 6 was obtained with the pseudo-isotropic

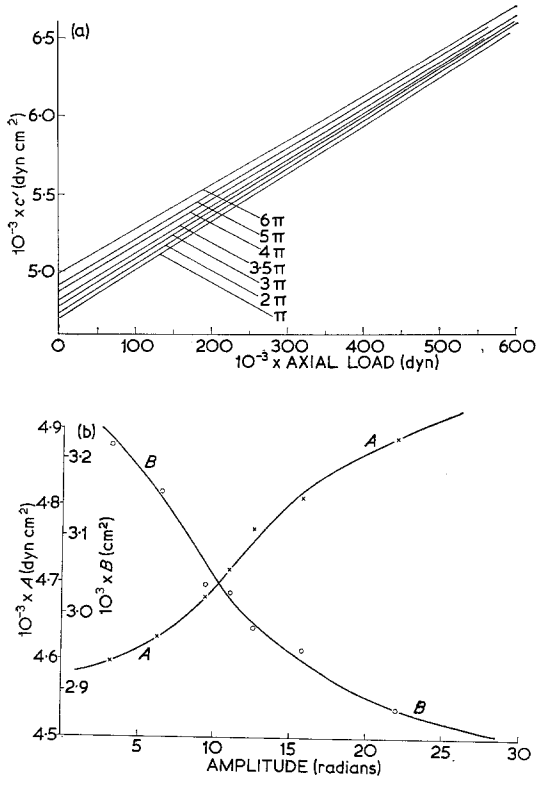

Figure 3 Calibration of suspension. (a) $c'(= A + BW)$ versus axial load (W); (b) A and B versus amplitude.

method and it shows $S_{55}{}^z$ and $S_{55}{}^x$ versus aspect ratio. The twist was 0.34 radians.

Assuming that an aspect ratio of 23 is sufficiently large for the pseudo-isotropic assumption to be realistic, we obtain:

$$\overline{S_{55}{}^z} = 5.09 \times 10^{-11}\ \text{cm}^2\ \text{dyn}^{-1},$$
$$\overline{S_{55}{}^x} = 7.85 \times 10^{-11}\ \text{cm}^2\ \text{dyn}^{-1}$$

and

$$\overline{S_{55}} = 6.47 \times 10^{-11}\ \text{cm}^2\ \text{dyn}^{-1}$$

where $\overline{S_{55}}$ is the average of $\overline{S_{55}{}^z}$ and $\overline{S_{55}{}^x}$.

Figs. 7a and b show the time-dependence of $\overline{S_{55}{}^x}$ and $\overline{S_{55}{}^z}$ respectively, using two samples of very large aspect ratio (where, in both cases, the S_{55} contribution to the St Venant relations is much larger than the contribution of S_{44} and S_{66} respectively). If ΔS is the time-dependence between 10 and 1000 sec, we define:

$$\Delta S = \frac{S_{1000\,\text{sec}} - S_{10\,\text{sec}}}{S_{10\,\text{sec}}} \times 100\% \cdot$$

The results show that $\overline{\Delta S_{55}{}^x} = 1.6\%$ and $\overline{\Delta S_{55}{}^z} = 2.0\%$.

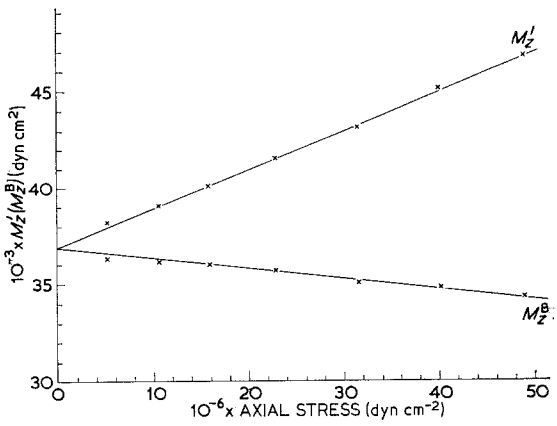

Figure 4 $S_{55}{}^z$ determination: M_z' and $M_z{}^B$ versus axial stress; M_z' = torque per unit twist per unit length of sample; $M_z{}^B$ = St Venant torque calculated with the Biot correction.

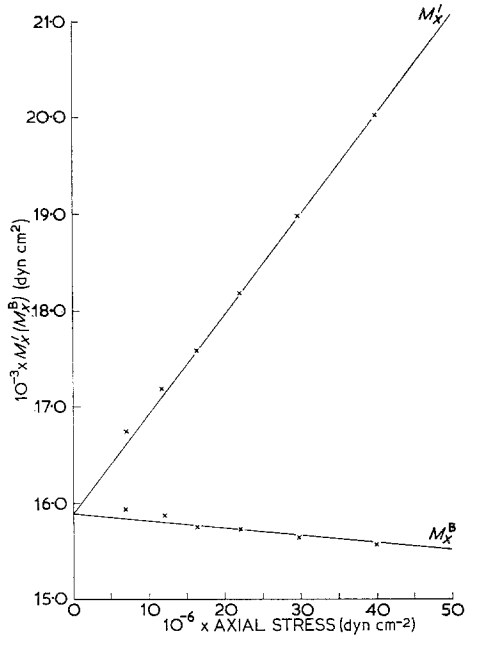

Figure 5 $S^x{}_{55}$ determination: M_x' and $M_x{}^B$ versus axial stress; M_x' = torque per unit twist per unit length of sample; $M_x{}^B$ = St Venant torque calculated with the Biot correction.

4.4. Calculation of S_{66} and S_{44}

The calculated values of $S_{66}{}^x$ and $S_{44}{}^z$ (as given by the St Venant relations for any aspect ratio) are shown in Fig. 8a and b respectively. Different curves are given for each of the calculated values of S_{55} ($\overline{S_{55}{}^z}$, $\overline{S_{55}{}^x}$ and $\overline{S_{55}}$). For aspect ratios

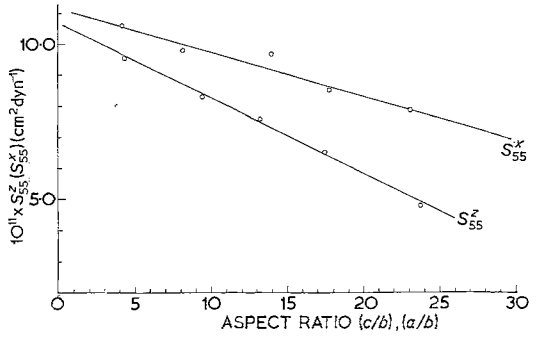

Figure 6 Plot of $S_{55}{}^{z}$ and $S_{55}{}^{x}$ versus aspect ratio (pseudo-isotropic method).

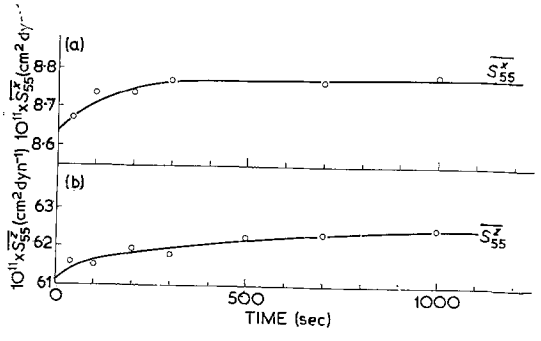

Figure 7 Shear compliances $\overline{S_{55}{}^{x}}$ and $\overline{S_{55}{}^{z}}$ as a function of time (a) $\overline{S_{55}{}^{x}}$ for aspect ratio $c/b = 21.6$, (b) $S_{55}{}^{z}$ for aspect ratio $a/b = 18.5$.

$c/b \to 0$ and $a/b \to 0$, all the curves converge towards the true values of S_{66} and S_{44} respectively. Averaging these extrapolations for each value of S_{55} we obtain

$$\overline{S_{66}{}^{x}} = 27.7 \times 10^{-11}\ \text{cm}^2\ \text{dyn}^{-1},$$
$$\overline{S_{44}{}^{z}} = 26.25 \times 10^{-11}\ \text{cm}^2\ \text{dyn}^{-1}.$$

4.5. Calculation of extensional compliances

Figs. 9 and 10 show the isochronous 10 sec stress-strain curves for S_{33} and S_{22} respectively. Because S_{33} is very small compared with S_{11}, the maximum extension in the z (draw) direction is 0.22%, compared with 0.85% in the x direction. Not surprisingly, S_{33} appears to be linear within the narrow range measured, whereas S_{11} can be seen to be appreciably non-linear at all levels of strain. The results at 10 sec and 0.1% strain are:

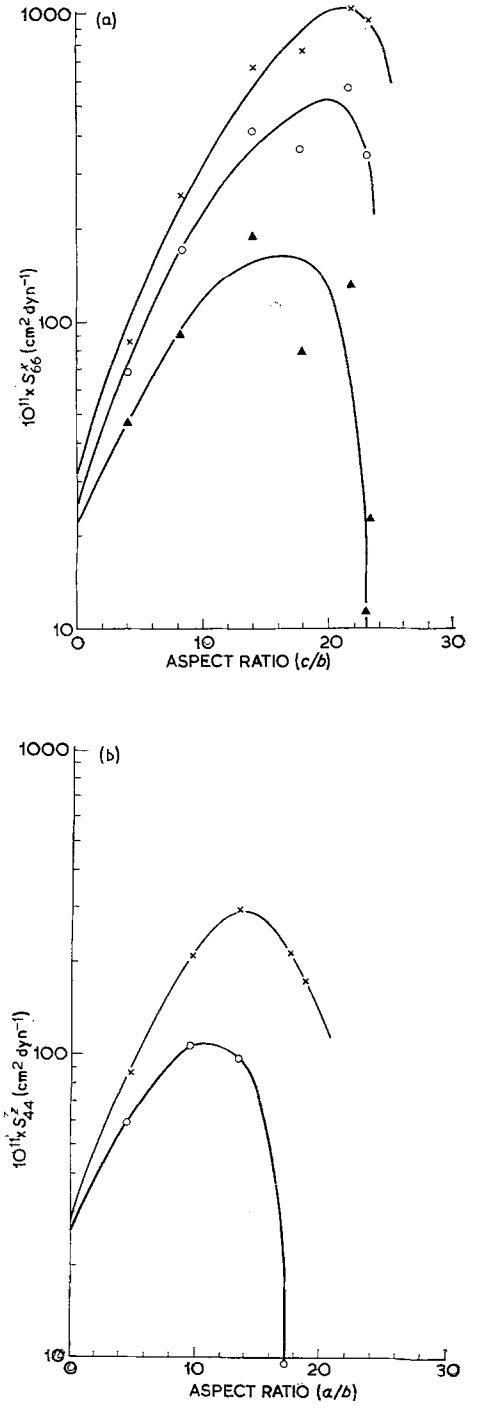

Figure 8 Calculation of S_{66} and S_{44} using the exact method.

Plots of $S_{66}{}^{x}$ (a) and $S_{44}{}^{z}$ (b) versus aspect ratio
× $S_{55} = \overline{S_{55}{}^{z}} = 5.09 \times 10^{-11}$ cm^2 dyn^{-1}
○ $S_{55} = \overline{S_{55}} = 6.47 \times 10^{-11}$ cm^2 dyn^{-1}
▲ $S_{55} = \overline{S_{55}{}^{x}} = 7.85 \times 10^{-11}$ cm^2 dyn^{-1}.

$$S_{33} = 0.58 \times 10^{-11}\ \text{cm}^2\ \text{dyn}^{-1},$$
$$S_{11} = 4.45 \times 10^{-11}\ \text{cm}^2\ \text{dyn}^{-1}.$$

The time-dependences between 10 and 1000 sec, as defined above, are $\Delta S_{33} = 3\%$, $\Delta S_{11} = 3\%$ and are shown in Fig. 11a and b respectively.

5. Discussion

5.1. Time-dependence

All the time-dependences measured (ΔS_{33}, ΔS_{11} and ΔS_{55}) are very small and do not appear to be of interest at present.

5.2. Determination of shear compliances

In Fig. 6 we see that both $S_{55}{}^z$ and $S_{55}{}^x$, calculated with the pseudo-isotropic method, are decreasing functions of the aspect ratio. Also $S_{55}{}^x > S_{55}{}^z$. This is the case (a_1) in the theoretical section which predicted that both S_{66} and S_{44} would be larger than S_{55}, and that $S_{66} > S_{44}$. These predictions are in complete agreement with the results, although it must be pointed out that the difference between S_{66} and S_{44} is within experimental error.

We would have expected both $S_{55}{}^z$ and $S_{55}{}^x$ to converge asymptotically towards the true value of S_{55} for large aspect ratios. The fact that the experimental curves are neither convergent nor asymptotic can be due to a combination of three adverse factors:

1. Variability along the sheet, which reflects itself in a variation of about 8% for S_{33}.

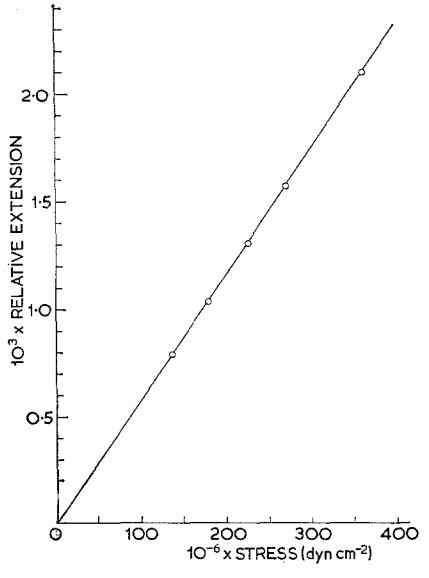

Figure 9 Calculation of S_{33} (10 sec). Relative extension versus stress.

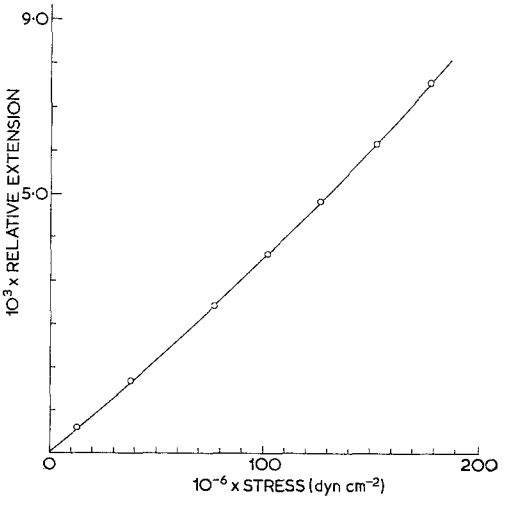

Figure 10 Calculation of S_{11} (10 sec.) Relative extension versus stress.

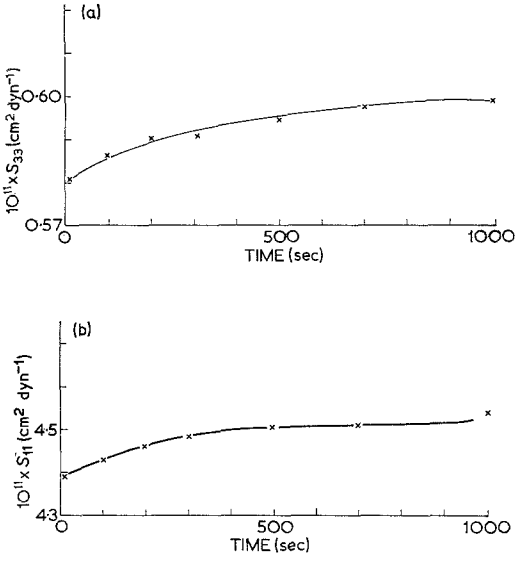

Figure 11 Extensional compliances S_{33} (a) and S_{11} (b) as a function of time.

2. The sheet is not perfectly orthorhombic.
3. Because $S_{66} \simeq S_{44} \gg S_{55}$ we are in the worst condition to calculate S_{55} with the pseudo-isotropic assumption. This applies for twist axes in both the z and x directions.

We have therefore considered three values of S_{55}, i.e. as before we consider $\overline{S_{55}{}^z}$, $\overline{S_{55}{}^x}$ and $\overline{S_{55}}$, all taken for an aspect ratio $c/b \simeq a/b \simeq 23$. We will show later that both $\overline{S_{55}{}^z}$ and $\overline{S_{55}}$ are reasonably near the true value.

We now consider the determination of S_{66} and S_{44}. We have seen in the theoretical part that, knowing S_{55}, the torsion experiments give:

$$\beta(u_x) = \frac{M_x S_{55}}{cb^3} \qquad \beta(u_z) = \frac{M_z S_{55}}{ab^3}$$

u_x and u_z are now calculated from Fig. 2 and finally

$$S_{66} = \left(\frac{c}{b}\right)^2 \frac{S_{55}}{u_x^2} \qquad S_{44} = \left(\frac{a}{b}\right)^2 \frac{S_{55}}{u_z^2}.$$

Table I gives the calculations used in Fig. 8a and b.

TABLE I Calculation of S_{44} and S_{66} for polyethylene terephthalate sheets D.R. = 5:1 at constant width.

(a) S_{66}

S_{55} (cm² dyn⁻¹ × 10¹¹)	M_x (dyn . cm² × 10⁻³)	cb^3 (cm⁴ × 10⁶)	$\beta(u_x)$	u_x	c/b	$S_{66}{}^x$ (cm² dyn⁻¹ × 10¹¹)
$\overline{S_{55}{}^z} = 5.09$	7.117	2.289	0.1583	1.138	8.1085	258.43
	12.221	3.716	0.1674	1.211	13.8962	669.99
	3.124	1.171	0.1358*	≃1*	4.1120	≃86.4*
	21.630	5.254	0.2095	1.673	23.0101	962.83
	15.890	4.216	0.1918	1.448	17.7400	763.89
	22.280	5.977	0.1897	1.427	21.6193	1168.45
$\overline{S_{55}} = 6.470$	7.117	2.289	0.2012	1.562	8.1085	174.34
	12.221	3.716	0.2128	1.723	13.8962	420.80
	3.124	1.171	0.1726	1.258	4.1120	69.12
	21.630	5.254	0.2664	3.130	23.0101	349.66
	15.890	4.216	0.2439	2.353	17.7400	367.74
	22.280	5.977	0.2412	2.293	21.6193	575.11
$\overline{S_{55}{}^x} = 7.85$	7.117	2.289	0.2441	2.368	8.1085	92.05
	12.221	3.716	0.2582	2.800	13.8962	193.35
	3.124	1.171	0.2094	1.671	4.1120	47.54
	21.630	5.254	0.3232	19.00	23.0101	11.51
	15.890	4.216	0.2959	5.82	17.7400	72.94
	22.280	5.977	0.2926	5.24	21.6193	133.62

* $\beta(u_x)$ slightly smaller than the lower limit.

(b) S_{44}

S_{55} (cm² dyn⁻¹ × 10¹¹)	M_z (dyn . cm² × 10⁻³)	ab^3 (cm⁴ × 10⁶)	$\beta(u_z)$	u_z	a/b	$S_{44}{}^z$ (cm² dyn⁻¹ × 10¹¹)
$\overline{S_{55}{}^z} = 5.09$	7.910	2.118	0.1901	1.430	9.4304	221.32
	16.625	3.972	0.2130	1.728	13.2479	299.18
	3.643	1.220	0.1520	1.087	4.4834	86.56
	36.900	5.414	0.3469	—	23.7100	—
	22.380	4.549	0.2504	2.545	17.3740	237.11
	31.220	5.971	0.2661	3.115	18.5157	179.85
$\overline{S_{55}} = 6.470$	7.910	2.118	0.2416	2.298	9.4304	108.95
	16.625	3.972	0.2708	3.340	13.2479	101.75
	3.643	1.220	0.1934	1.467	4.4834	60.43
	36.90	5.414	0.4410	—	23.7100	—
	22.38	4.549	0.3183	14.03	17.3740	9.92
	31.22	5.971	0.3383	—	18.5157	—
$\overline{S_{55}{}^x} = 7.85$	7.910	2.118	0.2932	5.38	9.4304	24.12
	16.625	3.972	0.3286	60.00	13.2479	0.38
	3.643	1.220	0.2537	2.640	4.4834	22.64
	36.90	5.414	0.5350	—	23.7100	—
	22.38	4.549	0.3862	—	17.3740	—
	31.22	5.971	0.4104	—	18.5157	—

We first note that the values of $\beta(u)$ obtained as above, must be within the narrow limits 0.145 to 0.330 to have physical meaning, i.e. to provide a value of u. The fact that only seven of the thirty-six calculations made from experiments in twelve samples fail to do so suggests that the values obtained for S_{55} are close to the true one. Three of these seven wrong values of $\beta(u)$ are for the calculation of S_{44} with $\overline{S_{55}^{x}} = 7.85 \times 10^{-11}$ cm^2 dyn^{-1} together with another value very nearly outside the higher limit. We can, therefore, assume that this $\overline{S_{55}^{x}}$ value is too high and that both $\overline{S_{55}^{z}}$ and $\overline{S_{55}}$ are more representative of the mechanical properties of the sheet. We finally take

$$S_{55} = \frac{\overline{S_{55}^{z}} + \overline{S_{55}}}{2} = 5.88 \times 10^{-11} \text{ cm}^2 \text{ dyn}^{-1}.$$

We have said elsewhere [3] that our method gives correct predictions only when the pseudo-isotropic assumption is a good approximation, that is, when the only shear compliance contributing to the twist is the one shown explicitly in the St Venant relation. Had we been able to calculate S_{66} and S_{44} with the pseudo-isotropic assumption (i.e. if we could have had comparable sheets of different thickness), the expressions would have been

$$M_x = \frac{bc^3}{S_{66}}\beta(u_x') \qquad u_x' = \frac{b}{c}\sqrt{\left(\frac{S_{66}}{S_{55}}\right)}$$

$$M_z = \frac{ba^3}{S_{44}}\beta(u_z') \qquad u_z' = \frac{b}{a}\sqrt{\left(\frac{S_{44}}{S_{55}}\right)}$$

and the correct results would have been obtained for

$$\frac{b}{c} \gg 1 \qquad \frac{b}{a} \gg 1. \tag{3}$$

Under these conditions it is clear that errors in S_{55} do not affect the results.

Because of the experimental impossibility of complying with the above conditions for the aspect ratios, we calculated S_{66} and S_{44} with the "exact" method and extrapolated the results to:

$$\frac{c}{b} \to 0 \text{ and } \frac{a}{b} \to 0 \tag{4}$$

which, of course, is mathematically equivalent to Relation 3. The "exact" method with Condition 4 will therefore give reasonable values of S_{66} and S_{44}, whatever the value assumed for S_{55}. These conclusions are supported by the experimental results shown in Fig. 8a and b where it is seen that the curves for $\overline{S_{55}^{z}}$, $\overline{S_{55}^{x}}$ and $\overline{S_{55}}$ all converge for aspect ratios toward zero, in spite of the fact that at other aspect ratios, the relative differences between them can be as large as two orders of magnitude. Further support for the suitability of the method used here for determining S_{66} and S_{44} will be given in a future paper.

5.3. Further comments on the application of the St Venant theory in these experiments

It is interesting to note that in Fig. 8a and b, both S_{66} and S_{44} first increase and then decrease with increasing aspect ratio. Table I shows that this decrease is always associated with an increase of the calculated $\beta(u)$ above certain values which are, in the calculations of S_{66}: 0.20 for $\overline{S_{55}^{z}}$, 0.24 for $\overline{S_{55}}$ and 0.29 for $\overline{S_{55}^{x}}$. In the calculations of S_{44} the critical values of $\beta(u)$ are: 0.20 for $\overline{S_{55}^{z}}$ and 0.25 for $\overline{S_{55}}$. These critical values not only apply to the trend of S_{66} and S_{44} versus aspect ratio, but also explain the observed scatter of the experimental points.

A similar effect was observed in previous shear compliance measurements of highly-drawn low-density polyethylene [3], although at that time the number of measurements were insufficient to attribute this effect to other than statistical errors. Fig. 12a shows a plot of these results, and Table II shows the calculations for the points obtained with the "exact" method (points marked with a circle "O" in Fig. 12a). These results are given in a co-ordinate system compatible with the one used in this paper, that is, the z-axis in the draw direction, the x-axis perpendicular to it and in the plane of the sheet, the y-axis perpendicular to the plane of the sheet. In this system the sheet is transversely isotropic in the xy plane, and $S_{44} = S_{55}$.

We can see that the two points with S_{66} below the interpolated curve are the only ones with the corresponding $\beta(u_x)$ larger than 0.23.

It is also necessary to consider that the stress distribution in these specimens may be affected by end conditions, and that the discrepancies arise from the use of short specimens [10]. Fig. 12b shows the calculated values of S_{66} using the exact method, as a function of the length/width ratio. Comparison of Fig. 12a and b suggests that the correlation is with the aspect ratio, rather than the length/width ratio. It can certainly be concluded that the calculation of the torque in these experiments using the St Venant theory

TABLE II Calculation of S_{66} for transversely isotropic low density polyethylene.

$S_{55} = S_{44}$ (cm^2 dyn^{-1} × 10^{11})	M_x (dyn . cm^2 × 10^{-3})	cb^3 (cm^4 × 10^5)	$\beta(u_x)$	u_x	c/b	$S_{66}{}^x$ (cm^2 dyn^{-1} × 10^x)
341	0.4031	0.860	0.1614	1.160	13.912	49260
490	2.387	5.090	0.2327	2.071	7.589	6631
490	1.541	3.989	0.1904	1.435	5.828	8117
513	1.771	3.665	0.2477	2.460	6.044	3094
490	1.142	2.895	0.1944	1.483	3.873	3357
490	0.5718	1.307	0.1996	1.540	2.074	893.4
508	2.923	7.479	0.1989	1.540	0.9574	191.2

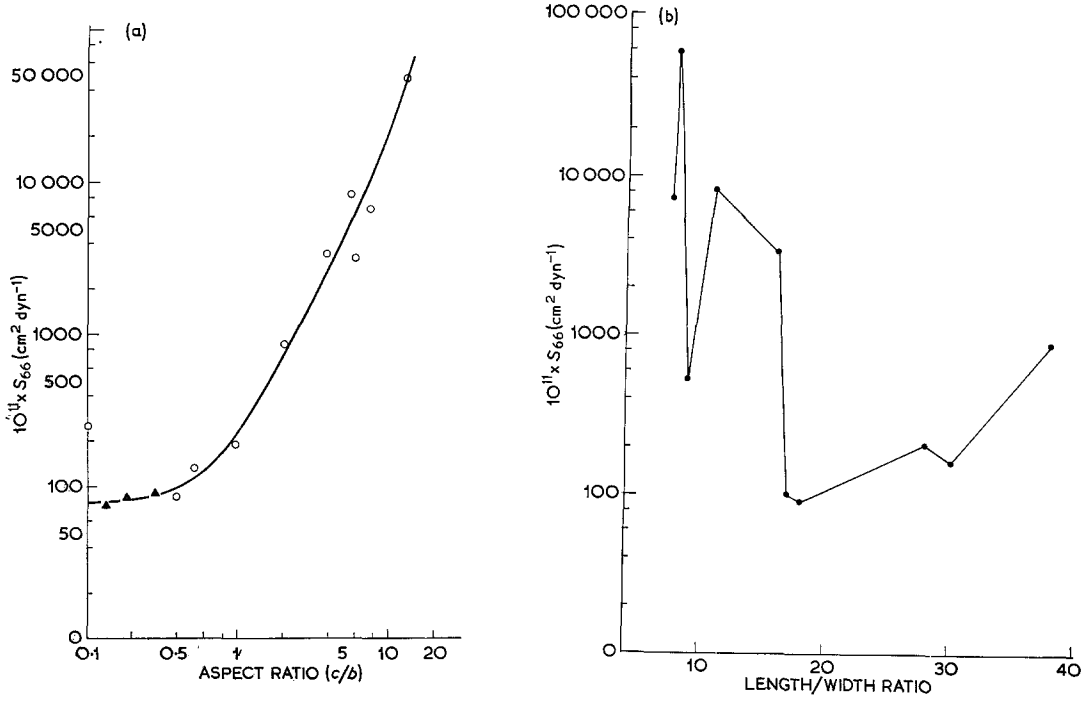

Figure 12 Uniaxially oriented low density polyethylene. (a) Plot of S_{66} versus aspect ratio from the exact (○) and semiexact (▲) methods [3]. (b) Plot of S_{66} versus length/width ratio.

for small strain elasticity with no elaboration, is not correct in the situation where two shear moduli contribute to the elastic behaviour, and that it is necessary to proceed by the empirical extrapolation procedure.

5.4. Physical interpretation of the results

The five measured elastic compliances are (all 10 sec compliances, S_{33} and S_{11} at 0.1 % strain)

$S_{33} = 0.58$ $S_{11} = 4.45$ $S_{66} = 27.7$
$S_{44} = 26.2$ $S_{55} = 5.88$

(all results in 10^{-11} cm^2 dyn^{-1}).

Fig. 13 shows, graphically, the relationship between the shear compliances, the system of cartesian co-ordinates, shear stresses and shear strains. The plane of the sheet is the zx plane and this contains the crystalline (100) planes. (These planes have the maximum atomic density.) It can be seen that both S_{66} and S_{44} do not involve deformation but displacement of the (100) planes, while S_{55} involves deformation of these planes. We see from the compliance results that $S_{66} \simeq S_{44}$ and moreover that $S_{66} \simeq 5S_{55}$. A straightforward explanation of these compliance results is that the planar orientation of the crystallites has a considerable stiffening effect in their (100) planes. A mechanism involving displacements and deformation of the whole crystals cannot be ruled out but, since small angle X-ray diffraction photographs showed no trace of lamellar morphology, and little is known about

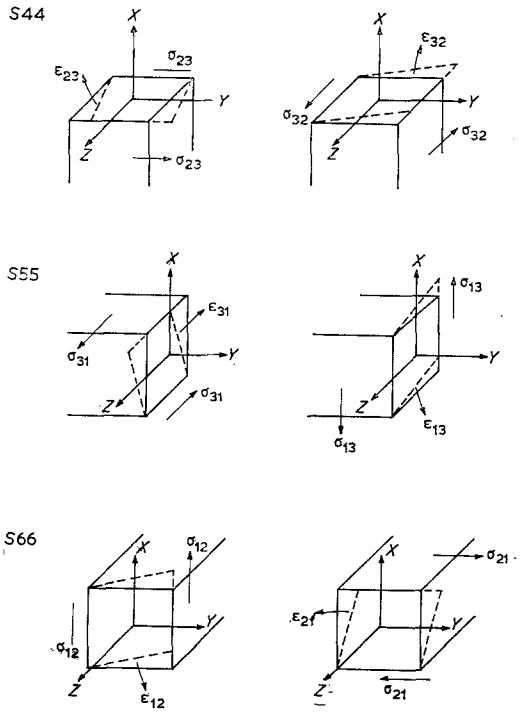

Figure 13 The relationships between the system of Cartesian co-ordinates, shear stresses and shear strains for the different shear compliances. (The plane of the sheet is the *zx* plane.)

the samples as a crystalline-amorphous composite no definitive conclusions can be reached about this possibility.

Both S_{33} and S_{11} also deform the (100) planes but they differ in that, while S_{11} can also separate the molecules in the (100) planes, S_{33} must stretch them in their orientation direction. Thus it is not surprising that $S_{11} \gg S_{33}$.

When making a quantitative comparison between extensional and shear compliances, we must use the matrix and not the tensor components (see Appendix). From the values quoted above their relationships are

$$S_{66} \simeq S_{44} \gg S_{55} > S_{11} \gg S_{33}$$

consistent with the plausible physical interpretation that the easiest deformation mechanism is the displacement of the (100) planes containing the benzene rings, followed by shear deformation of the (100) planes. Next in increasing difficulty is the lateral separation of the molecules in the (100) planes and finally a deformation of these planes, together with extension of the molecules in their orientation direction.

6. Conclusion

For the first time, the St Venant theory has been applied to determine the three shear compliances of a sheet with orthorhombic symmetry. In spite of the experimental difficulties produced by the availability of only one thin sheet, and the fact that the relationship between the shear compliances placed us in the worst situation for the application of the theory, the results obtained appear reliable and capable of physical interpretation.

Although only 35% of the material is crystalline, it has been suggested that the planar orientation of the (100) planes is a fundamental factor in determining the mechanical behaviour of the sheet.

Appendix

When studying the mechanisms contributing to extension and shear, it is often useful to have a quantitative comparison between extensional and shear compliances. In this case, it is necessary to decide whether the comparison should be made between the matrix components of the compliances (engineering compliances) or between their tensor components. The relationships are

$$S_{22} = S_{2222} \qquad S_{55} = 4S_{1313}$$

where S_{22} and S_{55} are matrix components and S_{2222} and S_{1313} are tensor components. We take them to illustrate the general procedure.

Hooke's law can be written in two different ways.

1. The engineering (or matrix) form

$$\begin{aligned}\epsilon_2 &= S_{21}\sigma_1 + S_{22}\sigma_2 + S_{23}\sigma_3 + S_{24}\sigma_4 \\ &\quad + S_{25}\sigma_5 + S_{26}\sigma_6 \\ \epsilon_5 &= S_{51}\sigma_1 + S_{52}\sigma_2 + S_{53}\sigma_3 + S_{54}\sigma_4 \\ &\quad + S_{55}\sigma_5 + S_{56}\sigma_6 .\end{aligned}$$

2. The tensorial form

$$\begin{aligned}\epsilon_{22} &= S_{2211}\sigma_{11} + S_{2222}\sigma_{22} + S_{2233}\sigma_{33} \\ &\quad + S_{2223}\sigma_{23} + S_{2232}\sigma_{32} + S_{2212}\sigma_{12} \\ &\quad + S_{2221}\sigma_{21} + S_{2213}\sigma_{13} + S_{2231}\sigma_{31} \\ \epsilon_{13} &= S_{1311}\sigma_{11} + S_{1322}\sigma_{22} + S_{1333}\sigma_{33} \\ &\quad + S_{1323}\sigma_{23} + S_{1332}\sigma_{32} + S_{1312}\sigma_{12} \\ &\quad + S_{1321}\sigma_{21} + S_{1313}\sigma_{13} + S_{1331}\sigma_{31} .\end{aligned}$$

All the engineering (or matrix) stresses are equivalent to the tensor stresses

$$\sigma_2 = \sigma_{22} \qquad \sigma_5 = \sigma_{13} = \sigma_{31} .$$

The engineering tensile strains are equivalent to the tensor tensile strains

$$\epsilon_2 = \epsilon_{22}$$

but the engineering shear strains are not equivalent to the tensor shear strains

$$\epsilon_5 = 2\epsilon_{13} = 2\epsilon_{31} .$$

ϵ_{22} is the displacement in the y direction of a point situated at a unit distance from the origin. ϵ_{13} is half the relative displacement in the direction of two planes perpendicular to z and separated by the unit distance (Fig. 14).

Therefore, from a physical standpoint, comparisons must be made between matrix, and not tensor components of strains, and similarly for the compliances.

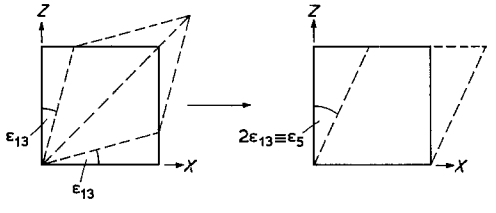

Fig. 14

Acknowledgement

N. H. Ladizesky's research for this paper was supported by the Science Research Council.

References

1. R. DE P. DAUBENY, C. W. BUNN, and C. J. BROWN, *Proc. Roy. Soc.* **226A** (1954) 531.
2. S. G. LEKHNITSKII, "Theory of Elasticity of an Anisotropic Elastic Body" (Holden-Day, San Francisco, California, 1963) p. 197.
3. N. H. LADIZESKY and I. M. WARD, *J. Macromol. Sci.* **B5** (1971) 745.
4. A. CAMPBELL, *Proc. Phys. Soc.* **25** (1913) 203.
5. H. PEALING, *Phil. Mag.* **25** (1913) 418.
6. J. C. BUCKLEY, *ibid* **28** (1914) 778.
7. H. A. BIOT, *J. Appl. Physics* **10** (1939) 860.
8. V. B. GUPTA and I. M. WARD, *J. Macromol. Sci.* **B1** (1967) 373.
9. N. H. LADIZESKY and I. M. WARD, *ibid* **B5** (1971) 661.
10. L. N. G. FILON, *Phil. Trans. Roy. Soc.* **198** (1902) 147.

Received 23 October and accepted 22 December 1972.